

The $SU(N)$ Heisenberg model on the square lattice: a continuous- N quantum Monte Carlo study

K. S. D. Beach*

Department of Physics, University of Alberta, Edmonton, Alberta, Canada T6G 2G7

Fabien Alet, Matthieu Mambrini, and Sylvain Capponi

*Laboratoire de Physique Théorique, Université de Toulouse, UPS, (IRSAMC), 31062 Toulouse, France and
CNRS, LPT (IRSAMC), 31062 Toulouse, France*

(Dated: December 18, 2008)

We present exact numerical results for the square-lattice $SU(N)$ Heisenberg model, computed using a singlet projector algorithm that is not restricted to integer values of N . Finite-size scaling of the data suggests a direct, continuous phase transition between a Néel-ordered phase and a crystalline bond-ordered phase at a single critical value $N_c = 4.57(5)$ with critical exponents $z = 1$ and $\beta/\nu = 0.81(3)$.

The field of quantum magnetism encompasses a large variety of physical phenomena that are of current experimental and theoretical interest. These include competition between interactions (frustration), ordering in conventional or unconventional magnetic states, and the existence of fractionalized excitations. In two dimensions, where some of the most unusual physics occurs, there is a conspicuous absence of methods for studying the behaviour of quantum magnets with high precision. On the analytical side, neither the powerful methods devised for dimension $d = 1$ (bosonization, conformal field theory) nor the mean-field methods applicable to $d > 3$ are available. On the numerical side, simulations are difficult because of the enormous size of the Hilbert space and, for stochastic methods, because of the fatal “sign problem.”

One way to relax these strong methodological constraints is to decrease the role of quantum fluctuations. For instance, considering the classical limit of magnets with large spin S eases both numerical and analytical studies. This limit, however, very often misses the important competition between the instabilities existing only at the quantum level. An alternative route—one that preserves the quantum fluctuations—is to enlarge the symmetry of the model, e.g., by extending the $SU(2)$ spin symmetry to $SU(N)$. This has proved very useful in the past, as the $N \rightarrow \infty$ limit often allows for an exact analytical treatment. Methods to study $1/N$ corrections are also available, although they cannot fully capture the exact details of what happens at finite N . The advantage of $SU(N)$ models over classical ones is that they naturally allow for quantum states of matter (such as valence bond solids) by construction, even if the off-diagonal elements of the Hamiltonian are suppressed in the large- N limit.

Using this technique, and building on previous work [1], Read and Sachdev [2] have studied in detail the $SU(N)$ generalization of the Heisenberg Hamiltonian on the square lattice. For sufficiently large N , the system spontaneously breaks lattice translation symmetry to form a valence bond crystal (VBC). For small N (in-

cluding the standard $SU(2)$ model at $N = 2$), the ground-state is antiferromagnetically ordered. The details of the phase diagram and of the VBC depend on the representation of the generators of the $SU(N)$ algebra considered: for the case of square Young tableaux with n columns, a direct phase transition between the Néel and VBC states is predicted to occur at the (mean-field) value $N/n \sim 5.26$.

In a technical breakthrough, Kawashima and coworkers [3, 4, 5] extended a quantum Monte Carlo (QMC) loop algorithm designed for $SU(2)$ models to the $SU(N)$ case (for all integer N and for all single-row Young tableaux). Studying the square lattice case with this exact numerical method, they found for $n = 1$ that the $N = 4$ model is Néel ordered, whereas the $N = 5$ model supports VBC order. This confirmed the analytical large- N predictions, but because of the discrete nature of the algorithm, these studies could not rule out an intermediate phase between $N = 4$ and 5. Even if this (possibly spin-liquid) phase does not exist, it is impossible to obtain a precise value for the critical parameter N_c separating the two phases and to ascertain the nature of the phase transition at N_c .

In this Letter, we introduce a novel algorithm, formulated in the total singlet basis, that can treat the parameter N continuously (in the manner of analytical, large- N techniques). Applying this approach to the square-lattice $SU(N)$ Heisenberg model, we find that there is a direct transition occurring at $N_c = 4.57(5)$ between the Néel and VBC columnar phases. The transition is found to be second order, with critical exponents $z = 1$ and $\beta/\nu = 0.81(3)$. At the end of the paper we discuss the implications of finding a second-order quantum phase transition between states with incompatible symmetries and the possible connection to the deconfined quantum criticality (DQC) scenario [6].

We consider the $SU(N)$ generalization of the Heisen-

berg model:

$$H = -J \sum_{\langle i,j \rangle} H_{ij} = \frac{J}{N} \sum_{\langle i,j \rangle} \sum_{\alpha,\beta=1}^N \mathcal{J}_\beta^\alpha(i) \mathcal{J}_\alpha^\beta(j), \quad (1)$$

where $J = 1$ sets the energy scale, $\langle i, j \rangle$ denotes nearest neighbor sites i and j , and \mathcal{J}_β^α are the generators of the $SU(N)$ algebra satisfying $[\mathcal{J}_\beta^\alpha(i), \mathcal{J}_{\beta'}^{\alpha'}(j)] = \delta_{ij}(\delta_{\alpha\beta'} \mathcal{J}_\beta^{\alpha'} - \delta_{\alpha'\beta} \mathcal{J}_{\beta'}^\alpha)$. We consider the “quark-antiquark” model, taking the fundamental representation of the generator for one sublattice (single-box tableau), and its conjugate ($N - 1$ boxes in one column) on the other sublattice. In that case, one can conveniently rewrite the model in terms of spin- S , $SU(2)$ moments on each site (with $N = 2S + 1$). The Hamiltonian can indeed be expressed with standard $SU(2)$ spin operators: for instance $H_{ij} = 1/4 - \mathbf{S}_i \cdot \mathbf{S}_j$ for $S = 1/2$ ($N = 2$), $H_{ij} = 1/3[(\mathbf{S}_i \cdot \mathbf{S}_j)^2 - 1]$ for $S = 1$ ($N = 3$), etc. This was the starting point of previous finite-temperature QMC investigations of this model [3, 4], where a path-integral technique was developed in the S_z basis of the spins [5]. Here we take a rather different route, using a $T = 0$ algorithm formulated in the $SU(2)$ total singlet basis of the spins S .

The Perron-Frobenius theorem shows that, on a bipartite finite lattice, Eq. (1) admits a unique [thus $SU(N)$ singlet] ground state. For general S , an $SU(2)$ singlet subspace can be formed by *bipartite valence bond* (VB) states [7] in which two spins S in opposite sublattices form a VB by coupling pairwise in a singlet [as in Fig. 1(a)], formally given in the S_z basis by $|\phi\rangle = (2S + 1)^{-1/2} \sum_{m=-S}^S (-1)^{m-S} |m, -m\rangle$. It is remarkable that H preserves this bipartiteness on the square lattice and that the ground-state can be expressed within this subspace. Moreover, we can impose a VB orientation convention such that the overlap between two states is positive. This basis is nonorthogonal, and the overlap between two VB states is $\langle \phi_1 | \phi_2 \rangle = (2S + 1)^{N_l - N_v}$, where N_l is the number of *loops* formed by superimposing the two VB states $|\phi_1\rangle$ and $|\phi_2\rangle$ and N_v is the total number of VBs. This is a simple generalization of the well-known overlap rule for $S = 1/2$.

It is crucial to remark that H_{ij} is a projector onto a local singlet for the two spins at sites i and j . As a consequence, the action of H_{ij} on VB states is extremely simple [8] and consists of the rearrangements depicted in Fig. 1(b). We already see at this stage that the value of the spin S (and of N) enters only (i) in the prefactor of the second update rule and (ii) in the overlap rule.

Noting that H is negative defined, we can apply the projector VB QMC developed by Sandvik [9] for $S = 1/2$, which works with such update rules. This method allows for an efficient sampling of the ground state of H . What remains is to determine how to compute observables. It is well-known in the $S = 1/2$ case that most observables can be written in terms of estimators based

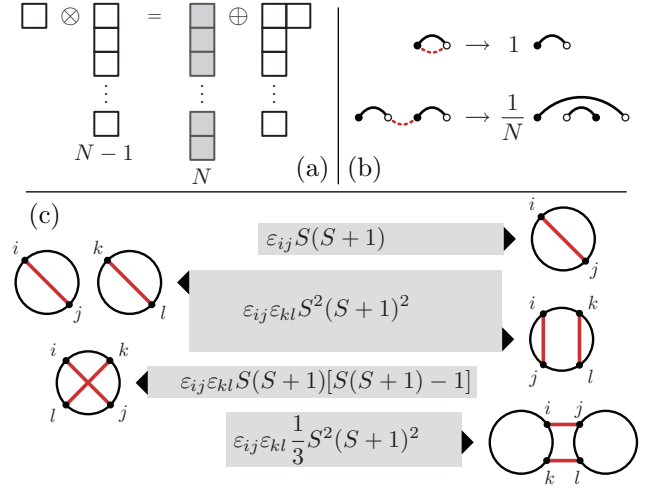


FIG. 1: (color online) (a) An A-sublattice and a B-sublattice spin can pair to form a singlet, which corresponds to a column of zero (modulo N) boxes. (b) Update rules for the action of H_{ij} on VB singlet states. (c) Loop diagrams contributing to two- and four-spin correlators (respectively $\mathbf{S}_i \cdot \mathbf{S}_j$ and $(\mathbf{S}_i \cdot \mathbf{S}_j)(\mathbf{S}_k \cdot \mathbf{S}_l)$) and their contributions. These overlap loops (schematically circular here) are obtained by superimposing the VB configurations $|\phi_1\rangle$ and $|\phi_2\rangle$. The straight (red) lines link the corresponding spins of the correlation function. Only diagrams with non-vanishing contributions are displayed.

on the overlap loops [7]. For instance, the spin correlator $\langle \phi_1 | \mathbf{S}_i \cdot \mathbf{S}_j | \phi_2 \rangle / \langle \phi_1 | \phi_2 \rangle = 3/4 \epsilon_{ij}$ if spins i and j belong to the same loop, 0 otherwise. Here $\epsilon_{ij} = 1$ if i and j are on the same sublattice, -1 otherwise. We have generalized these rules for the spin S case, and the resulting non-vanishing loop diagrams are given in Fig. 1(c), alongside the value of their contribution. With these formulae, we can easily calculate, e.g., the staggered magnetization and its powers or the VBC order parameter. The spin gap Δ_s can also be computed using the same triplet propagation technique introduced for the $S = 1/2$ case [7, 9].

We now make our key observation: since the update rules, the Monte Carlo weights, and the estimators have analytical expressions in N (or S), simulations can be performed for *arbitrary, continuous values of N* . Formally, this can be understood as an analytic continuation from integer to real N . This is a great advantage over other QMC techniques [5], which are restricted to half-integer and integer S . Large- N analytical techniques [2] can also treat continuous values of N , but our numerical technique allows for an *exact* treatment of the Hamiltonian, in contrast to the mean-field approximation inherent to the large- N approach. We should point out that the update rules are simple and sign-problem-free only because Eq. (1) is a pure, local-singlet projector. Our algorithm does not apply to general spin- S Hamiltonians.

We proceed by presenting our results for the square lattice $SU(N)$ model. Fig. 2 shows the square of the staggered magnetization and its Binder cumulant. It is

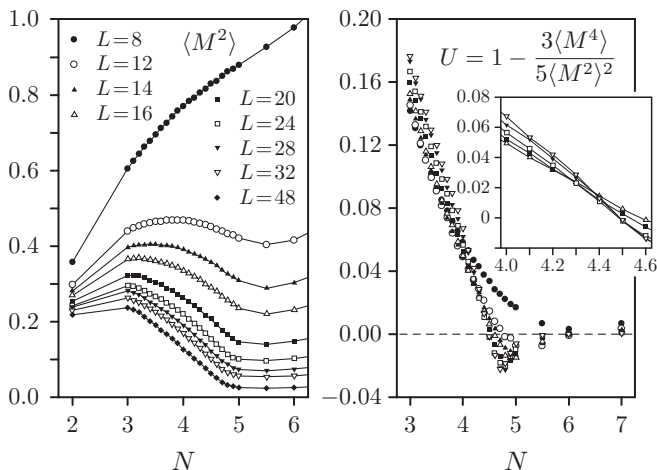


FIG. 2: (Left panel) Square of the staggered magnetization $\mathbf{M} = \frac{1}{L^2} \sum_{\mathbf{r}} (-1)^{r_x+r_y} \mathbf{S}_{\mathbf{r}}$ as a function of N for systems up to linear size $L = 48$ (lines are guides to the eye). (Right panel) The Binder cumulant U measures the kurtosis of the staggered magnetization with respect to a purely Gaussian distribution. It vanishes in the limit $L \rightarrow \infty$ in the absence of antiferromagnetic order.

apparent that in the thermodynamic limit a dome of antiferromagnetic order survives for $2 \leq N < N_c$ with N_c between 4 and 5. The Binder cumulant U has a crossing point at $N \approx 4.3$ which drifts rightward as L increases. We do not have data on sufficiently large systems to ascertain that the crossing is stable and can unambiguously be identified as the critical point. Moreover, U behaves unusually in a small region where its value is negative (excess kurtosis). This is sometimes a signature of a first-order transition or of a distribution with a complicated multi-peaked structure. We have verified that the distribution of staggered magnetization values is single-peaked and evolves smoothly across the transition. The negative region seems to correspond merely to a region in which the distribution is super-Gaussian. The width of this negative region vanishes in the thermodynamic limit.

The destruction of the Néel order is driven by the gradual elimination of singlet pairs that are correlated over long distances. In the large- N phase, the singlets are predominantly short-ranged and form domains of columnar ordering, corresponding to the order parameter $D_a = \frac{1}{L^2} \sum_{\mathbf{r}} (-1)^{r_a} \mathbf{S}_{\mathbf{r}} \cdot \mathbf{S}_{\mathbf{r}+\hat{\mathbf{e}}_a}$ for $a = x, y$ (see Fig. 3). On small lattices, these ordered domains are weak and they are almost equally distributed among the four degenerate configurations. This can be seen in the ring-like structure of the probability distribution $P(D_x, D_y)$, shown in Fig. 4, that appears for $N > N_c$. Previous work [3, 4] established the existence of VBC order for $N \geq 5$, but could not determine whether it was of columnar [$\langle \mathbf{D} \rangle \sim (0, \pm D), (\pm D, 0)$] or plaquette [$\langle \mathbf{D} \rangle \sim (\pm D, \pm D)$] symmetry. Our results suggest the former. There does not appear to be a true $U(1)$ degen-

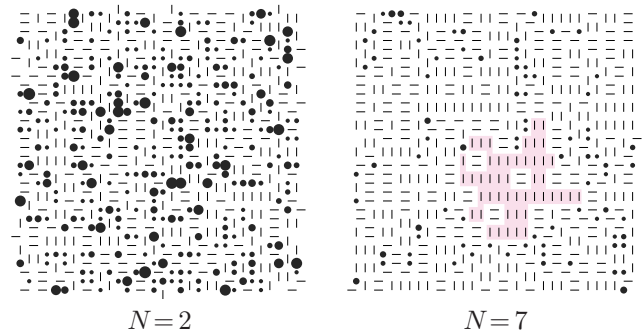


FIG. 3: (color online) Snapshots of typical VB configurations for a system of size $L = 32$. Short, nearest-neighbour bonds are drawn with a line; long bonds are indicated by circles (whose area is proportional to bond length) at their end points. For $N < N_c$, many long bonds stretch across the system. For $N > N_c$, short bonds dominate. The shaded (pink) area marks a crystal domain with columnar bond order.

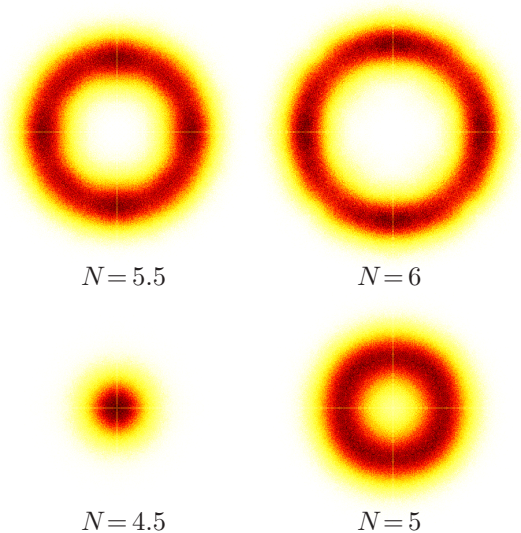


FIG. 4: (color online) Density plots of histograms $P(D_x, D_y)$ of the x - and y - components of the dimer order parameter ($L = 32$). On the magnetic side of the transition (e.g., $N = 4.5 < N_c$), the distribution is characterized by a central peak. On the VBC side, the distribution is ring-like but develops additional weight along the main axes as N is increased.

eracy, as suggested in Ref. 3. Instead, it seems that there is an additional length scale ξ_{VBC} much larger than the spin correlation length ξ . For $\xi < L < \xi_{\text{VBC}}$, there is merely an effective $U(1)$ degeneracy.

We have verified that the spin gap Δ_s vanishes as $1/L$ at the critical point, indicating that the dynamical critical exponent of the phase transition is $z = 1$. A finite-size scaling analysis of the magnetization and dimer order parameters suggests a continuous transition defined by a single critical value N_c and single set of critical exponents (see Fig. 5). The data are not sufficiently sensitive to fix

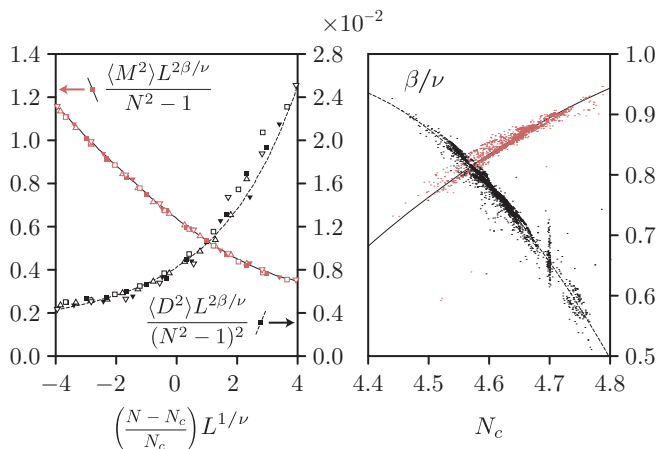


FIG. 5: (color online) Simultaneous data collapse of the Néel and dimer correlations can be achieved with a single set of critical exponents. The left panel shows the QMC measurements plotted in rescaled coordinates with the values $\nu = 0.88$, $\beta = 0.71$, and $N_c = 4.57(5)$. Other values of $\beta/\nu \sim 0.8$ produce good data collapse. The right panel shows bootstrapped results of β/ν versus N_c when fits of M^2 and D^2 are performed independently. A single critical point corresponds to the crossing $\beta/\nu = 0.81(3)$ and $N_c = 4.57(5)$.

the exponent ν precisely, and the unusual behaviour of the Binder cumulant—its negative region and strong sub-leading corrections—makes it unreliable for obtaining an independent estimate of ν . Reasonable fits seem to be achievable for a range of values $0.75 \lesssim \nu \lesssim 1$. On the other hand, the ratio β/ν is relatively stable. Repeating our fitting procedure for M^2 and D^2 independently with 3000 bootstrap samples, we conclude that both quantities vanish simultaneously and continuously at $N_c = 4.57(5)$ with $\beta/\nu = 0.81(3)$. Note that the anomalous dimension $\eta = 2\beta/\nu - 1 = 0.63(4)$ is at least an order of magnitude larger than what would be expected from either the 3D $O(3)$ or \mathbb{Z}_4 universality classes.

In conclusion, we have introduced an algorithm to simulate Heisenberg $SU(N)$ models (for the representation with a single row and column on one sublattice and its conjugate on the other) on any bipartite lattice. It is formulated in the total singlet sector and allows for efficient computations for arbitrary, continuous values of N . For the square lattice model, we find a second-order phase transition between a Néel and VBC columnar state at $N_c = 4.57(5)$. Constructing a Ginzburg-Landau theory for this phase transition is not simple from the symmetry point of view, as the external parameter N of the $SU(N)$ symmetry is tuned artificially to unphysical values in our numerics. Naively, the ingredients seem similar to those encountered in DQC points [6, 10]: a continuous Néel-VBC transition, driven by an external parameter that favors short VBs of the VBC over the long VBs needed for magnetic ordering. Strictly speaking, the arguments

of Ref. 6 do not apply here, since they rely heavily on Berry phase effects specific to $S = 1/2$. Hence, our results are not directly related to those of Refs. 6, 10. The large- N techniques of Ref. 2 do predict a continuous transition from Néel order to disorder, but the ground state degeneracy can only be computed for integer N . As far as we know, estimates of the critical exponents [11] are available only for representations with $n \gg 1$ and not beyond order $1/N$ and thus not useful for comparison with our numerical results.

Finally, we note that the algorithm presented here can be applied with minor modifications to the case of Heisenberg models with another generalized symmetry, namely $SU(2)_k$. This opens the door to the numerical study of topological quantum liquids, as found in Ref. 12.

We thank K. Harada and N. Kawashima for fruitful exchanges. Some calculations were performed using the ALPS libraries [13]. We thank IDRIS and CALMIP for allocation of CPU time. Support from the Procope (Egide) and French ANR programs (FA, MM and SC) and from the Alexander von Humboldt foundation (KSDB) is acknowledged.

* Electronic address: kbeach@phys.ualberta.ca

- [1] D. P. Arovas and A. Auerbach, Phys. Rev. Lett. **61**, 617 (1988); Phys. Rev. B **38**, 316 (1988).
- [2] N. Read and S. Sachdev, Phys. Rev. Lett. **62**, 1694 (1989); Nucl. Phys. **B316**, 609 (1989); Phys. Rev. B **42**, 4568 (1990).
- [3] N. Kawashima and Y. Tanabe, Phys. Rev. Lett. **98**, 057202 (2007).
- [4] K. Harada, N. Kawashima and M. Troyer, Phys. Rev. Lett. **90**, 117203 (2003).
- [5] N. Kawashima and K. Harada, J. Phys. Soc. Jap. **73**, 1379 (2004).
- [6] T. Senthil *et al.*, Science **303**, 14940 (2004); Phys. Rev. B **70**, 144407 (2004); J. Phys. Soc. Jpn. Suppl. **74**, 1 (2005).
- [7] K. S. D. Beach and A. W. Sandvik, Nucl. Phys. B **750**, 142 (2006).
- [8] I. Affleck, J. Phys.: Condens. Matter **2**, 405 (1990).
- [9] A. W. Sandvik, Phys. Rev. Lett. **95**, 207203 (2005).
- [10] O. I. Motrunich and A. Vishwanath, Phys. Rev. B **70**, 075104 (2004); A.W. Sandvik, Phys. Rev. Lett. **98**, 227202 (2007); R.G. Melko *et al.*, *ibid.* **100**, 017203 (2008); F.-J. Jiang *et al.*, J. Stat. Mech. P02009 (2008).
- [11] B. I. Halperin, T. C. Lubensky, and S.-K. Ma, Phys. Rev. Lett. **32**, 292 (1974); V. Y. Irkhin, A. A. Katanin, and M. I. Katsnelson, Phys. Rev. B **54**, 11953 (1996).
- [12] A. Feiguin *et al.*, Phys. Rev. Lett. **98**, 160409 (2007).
- [13] F. Albuquerque *et al.*, J. Magn. Mater. **310**, 1187 (2007); M. Troyer, B. Ammon and E. Heeb, Lecture Notes in Comput. Sci., **1505**, 191 (1998); see <http://alps.comp-phys.org>.